

Product Yields and Kinetics of Biomass Fast Devolatilization: Experiments and Modeling

Olivier Authier^{a*}, Benjamin Cluet^{b,c,d}, Arnaud Delebarre^c, Guillaïn Mauviel^d

^aEDF R&D, Fluid Dynamics Power Generation and Environment Department, 6 quai Watier, 78400 Chatou, France

^bLERMAB, 27 rue Philippe Séguin, CS 60036 88026 Épinal cedex, France

^cLEMETA-CNRS, 2 avenue de la forêt de Haye, 54500 Vandœuvre-lès-Nancy, France

^dLRGP-CNRS, 1 rue Grandville, 54000 Nancy, France

olivier.authier@edf.fr

The fast devolatilization of biomass is the first step of thermochemical conversion in fluidized bed boilers or gasifiers. Some advanced devolatilization models applicable to a wide range of biomasses and process conditions have been developed on the basis of a detailed description of the physico-chemical mechanisms and of biomass standard analysis. In this study, the results of a biomass devolatilization model taking into account the main physical and chemical phenomena are reported. Attention is focused on biomass thermal properties derived from its composition and density. The kinetic scheme is based on the lumped kinetic model of (Ranzi et al., 2008) and its further development. Predictions of the complete devolatilization time of biomass thick particles are compared with experimental results obtained in different high-temperature fluidized bed reactors. Experimental results obtained with biomass pellets under image furnace conditions are also used to assess the dynamic release of volatile matter predicted in transient state. The great interest of predictive model able to reduce the number of input parameters for any biomass type is finally underlined.

1. Introduction

The fast devolatilization of biomass is the first step of thermochemical conversion in fluidized bed boilers or gasifiers. The devolatilization complexity results mainly from biomass properties and composition, heating conditions, surrounding gas atmosphere and residence time distribution. The biomass conversion efficiency is controlled or altered by devolatilization kinetics and selectivity, i.e. product distribution (volatile matter: light gaseous species and tar, and char: solid residue). Consequently, the numerical prediction of multi-phase and multi-scale biomass devolatilization is still of importance for accurate simulation and optimization of biomass boiler or gasifier performance (gas heating value, tar content and composition, etc.).

Some advanced devolatilization models applicable to a wide range of biomasses and process conditions have been developed on the basis of a detailed description of the physico-chemical mechanisms and of biomass standard analysis, e.g. biochemical composition (Niksa, 2000) also including chemical percolation (Sheng and Azevedo, 2002) and kinetics studies (Ranzi et al., 2008). One of the main chemical kinetic model aiming to simulate both devolatilization kinetics and product distribution in any devolatilization conditions is the lumped kinetic scheme of Ranzi et al. based on multistep pseudo-reactions of the three main biomass components, i.e. cellulose, hemicellulose and lignin. However, due to the large size of biomass chips/pellets (mm to cm) in fluidized bed, devolatilization models need an appropriate coupling between chemical kinetics and transport phenomena, e.g. because of important temperature gradients inside the particles. Therefore, the resulting model needs also to include the biomass thermal properties (e.g. heat capacity, thermal conductivity) that are often badly known, especially when they evolve at high temperatures.

In this study, the results of a biomass devolatilization model taking into account the main physical and chemical phenomena are reported. Attention is focused on dry biomass properties derived from its

composition and density. Two types of facilities at the laboratory scale are taken into consideration: bubbling fluidized bed reactors and an image furnace (i.e. biomass heating by a concentrated radiation and volatile matter quenching in an inert gas at room temperature).

In a first part, predictions of the complete devolatilization time and char yield are compared, as a function of biomass initial diameter and bed temperature, with experimental results obtained in different high-temperature bubbling fluidized bed reactors.

In a second part, experimental results obtained with biomass pellets under image furnace conditions are used to assess the dynamic release of volatile matter predicted in transient state. The experimental mass loss and gas composition are then compared to model predictions.

2. Fast devolatilization modeling in thermally thick regime

2.1 Dimensionless numbers analysis

Biomass devolatilization can be controlled by chemical reactions, mass and energy transport phenomena through a porous media. If the rate-controlling phenomena are not identified, mathematical models have to take into account complex coupling between conservation of mass, momentum and energy. To a first approximation, the Peclet (Pe), Lewis (Le) and Biot (Bi) dimensionless numbers (Authier et al., 2009) are used to define the devolatilization regime of spherical biomass particles between 2 to 40 mm under fluidized bed conditions (Table 1). Such an analysis derived from a characteristic time analysis is qualitative because many parameters vary during devolatilization.

The values of Pe, Le and Bi show that internal heat transfer is rate-controlling during devolatilization of thick biomass particles under fluidized bed conditions. Hence, the knowledge of biomass thermal properties and their evolution with temperature can improve the results of fast devolatilization modeling in thermally thick regime.

Table 1: Dimensionless numbers used for devolatilization regime analysis

Dimensionless number	Ratio of characteristic times	Expression	Order of magnitude	Parameters
Peclet (Pe)	$\frac{\tau_{\text{mass diffusion}}}{\tau_{\text{mass convection}}}$	$\frac{P_G K}{D_{\text{eff}} \mu_G}$	$\gg 1$	$P_{G[Pa]} \cong 10^5$
				$K_{[m^2]} \cong 10^{-14} - 10^{-12}$
				$D_{\text{eff}[m^2.s^{-1}]} \cong 10^{-6}$
				$\mu_{G[Pa.s]} \cong 10^{-5}$
Lewis (Le)	$\frac{\tau_{\text{mass convection}}}{\tau_{\text{internal heat transfer}}}$	$\frac{\mu_G \lambda_{\text{eff}}}{P_G K \rho C_p}$	$\ll 1$	$\lambda_{\text{eff}[W.m^{-1}.K^{-1}]} \cong 0.05 - 0.5$
				$\rho_{[kg.m^{-3}]} \cong 200 - 800$
				$C_p[J.kg^{-1}.K^{-1}] \cong 1000 - 2000$
Biot (Bi)	$\frac{\tau_{\text{internal heat transfer}}}{\tau_{\text{external heat transfer}}}$	$\frac{hL}{\lambda_{\text{eff}}}$	$\gg 1$	$h_{[W.m^{-2}.K^{-1}]} \cong 100 - 500$
				$L_{[m]} \cong 0.001 - 0.02$

2.2 Modeling of heat capacity

The heat capacity of biomass and char is calculated according to the coal model of (Merrick, 1983) based on the Einstein form of the quantum theory of solids, generalized by (Coimbra and Queiroz, 1995) and extrapolated to biomass properties.

Comparison with several independent measurements and modelling (Figure 1) shows that this model can be used quite satisfactorily to calculate the heat capacity of pure biomass and char from their representative proximate and ultimate composition.

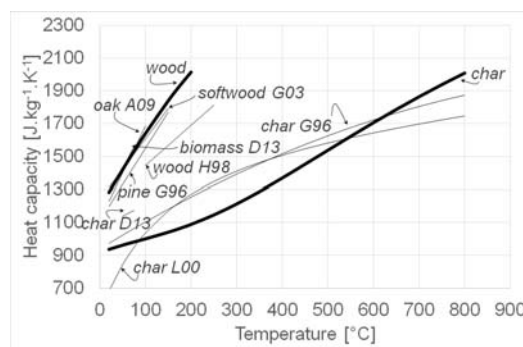


Figure 1: Heat capacities of different biomasses and chars as a function of temperature (thin lines: literature – G96 (Gronli, 1996), H98 (Harada et al., 1998), L00 (Larfeldt et al. 2000), G03 (Gupta et al. 2003), A09 (Authier et al. 2009), D13 (Dupont et al. 2013), thick lines: Merrick extrapolated model)

2.3 Modeling of thermal conductivity

The effective thermal conductivity can be estimated by the general formulation of (Thunman and Leckner, 2002) developed for wood thermal conversion and based on biomass fibrous structure defined as a system of serial and parallel conduction paths. This model that includes a radiative contribution at high temperature is mainly related to density and shrinkage parameters.

Details on calculation of effective thermal conductivity perpendicular and parallel to the fibres can be found in (Thunman and Leckner, 2002).

2.4 Fast devolatilization modelling

A one-dimensional model taking into account the main biomass physical and chemical phenomena and derived from previous studies (Authier et al., 2009) is applied to the conditions of fast devolatilization. The kinetic scheme is based on the last version of (Ranzi et al. 2014) lumped kinetic model. The boundary conditions at the particle surface are defined according to the reactor type, i.e. fluidized bed and image furnace. The average external heat transfer coefficient under fluidized bed conditions is calculated from the study of (Agarwal, 1991). The thermal conditions in image furnace are detailed in (Authier et al., 2009). The modelling approach aims for a detailed description of product yields and release rates estimated from biomass standard analysis. Properties of oak are used as a reference for modelling (Table 2).

Table 2: Typical properties of oak wood (CELL: cellulose $C_6H_{10}O_5$, HCE: hemicellulose $C_5H_8O_4$, LIGC: carbon-rich lignin $C_{15}H_{14}O_4$, LIGH: hydrogen-rich lignin $C_{22}H_{28}O_9$ and LIGO: oxygen-rich lignin $C_{20}H_{22}O_{10}$)

CELL	HCE	LIGC	LIGH	LIGO	C	H	O	Density
%wt dry ash free					%wt dry ash free			$kg \cdot m^{-3}$
51.1	27.8	3.2	2.9	15.1	47.8	5.4	46.8	550-760

3. Fast devolatilization under fluidized bed conditions

3.1 Experiments

A lot of experiments have been conducted to determine the total devolatilization time in bubbling fluidized bed reactors by techniques of flame extinction time, continuous gas analysis or pressure measurements (Table 3). Experiments have been carried out at different bed temperatures, fluidizing medium and velocities, biomass and bed material properties, i.e. composition, size, density, shape (spherical, cylindrical, cubic or irregular). In bubbling regime, fluidizing velocities vary generally from 5 up to 10 times the minimum fluidizing velocity. The correlations of devolatilization time are given in different forms like power-law expression as a function of biomass initial size, shape factor and bed temperature. The correlations are often given within an error band of $\pm 20\%$. The devolatilization time increases generally with the decrease of bed temperature and with the increase of biomass initial size.

The char yield defined as the ratio of final mass to the initial dry biomass mass has been also measured in several studies under fluidized bed conditions (Aarsen, 1985; Rapagna and Celso, 2008; Sreekanth and Kolar, 2010; Sudhakar and Kolar, 2011). The char yield appears to be slightly higher for lower bed temperatures. Several studies conclude a relatively low effect of biomass particle size on char yield. It can

also be pointed out that the effect of particle fragmentation is generally negligible before the final quarter of the devolatilization (Sudhakar and Kolar, 2011).

Table 3: Devolatilization time of different spherical biomass particles (shape factor equal to 1) under fluidized bed conditions (diameter: d_0 [mm], bed temperature: T [K])

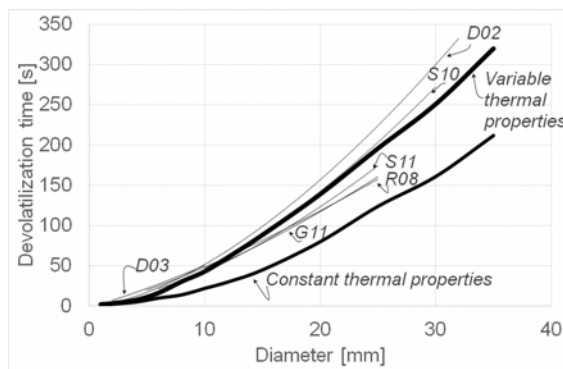
Devolatilization time (s)	Conditions	Reference
$1.03d_0^{1.6}$	Pine wood, 5 – 32 mm 850°C	De Diego et al. (2002) D02
$0.8\exp(1525/T)d_0^{1.2}$	Beech wood, 2 – 10 mm 534 – 834°C	Di Blasi and Branca (2003) D03
$2.514d_0^{0.94\exp(352/T)}$	Wood, 5 – 25 mm 700 – 900°C	Rapagna and Di Celso (2008) R08
$62d_0^{1.6}T^{-0.564}$	Wood, 10 – 30 mm 750 – 950°C	Sreekanth and Kolar (2010) S10
$18d_0^{1.548}T^{-0.389}$	Wood, 10 – 25 mm 750 – 950°C	Sudhakar and Kolar (2011) S11
$\exp(1013.2/T^{1.076})d_0^{1.414}$	White oak, 6 – 25 mm 500 – 900°C	Gaston et al. (2011) G11

3.2 Modeling

Despite the differences in experimental setups, operating conditions and/or methods of devolatilization time measurement, Figure 2.a shows that devolatilization time at a given temperature is controlled by the biomass initial size. The increase of devolatilization time with size is mainly due to higher resistance to internal heat transfer controlling the progress of devolatilization front from the particle surface to its center. It can be assumed that the thermal properties of biomass do not change with temperature. In this case, constant realistic values of $1300 \text{ J.kg}^{-1}.\text{K}^{-1}$ (heat capacity) and $0.15 \text{ W.m}^{-1}.\text{K}^{-1}$ (thermal conductivity) at room temperature are used for modelling. The theoretical devolatilization time is then greatly underestimated (curve “Constant thermal properties” on Figure 2.a) comparatively to the theoretical case with variable thermal properties.

Figure 2.b shows the final char yield as a function of biomass initial size and at different bed temperatures. Experimental char production increases slightly with increasing particle size and decreases with increasing bed temperature. The theoretical char trends do not agree very well with the experimental observations (Aarsen, 1985; Rapagna and Di Celso, 2008; Sreekanth and Kolar, 2010; Sudhakar and Kolar, 2011). However, the order of magnitude of theoretical char yield seems to be quite well predicted.

a. Devolatilization time at 850°C for different spherical biomass particles



b. Char yield for different biomass particles and bed temperatures

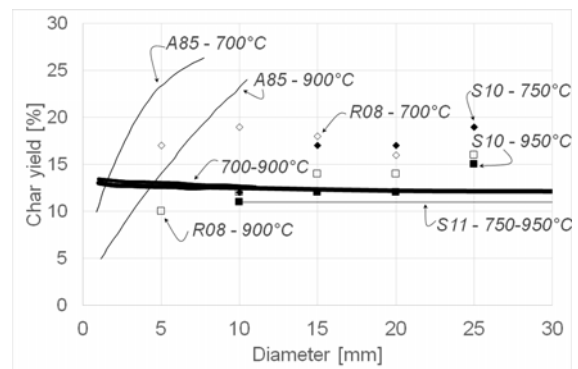


Figure 2: Results under fluidized bed conditions (thin lines: literature, thick lines: model results)

4. Fast devolatilization under image furnace conditions

4.1 Experiments

The image furnace relies on the use of concentrating mirrors associated to a high power discharge lamp adjusted at the first focus of an elliptical mirror (Authier et al. 2009; Authier and Lédé, 2013). The biomass pellet is placed at the second focus of this mirror inside a transparent walls reactor fed by nitrogen. Only the pellet is heated, but neither the reactor wall nor gas. The primary reaction species are quenched as soon as they leave the pellet. So, the secondary reactions in gas phase are prevented.

The thermal operating conditions in the image furnace are chosen as being close to those prevailing in a dual fluidized bed process (available heat flux density between $\phi_1 = 0.55 \text{ MW.m}^{-2}$ to $\phi_2 = 0.85 \text{ MW.m}^{-2}$). One of the pellet end cross section is submitted during controlled times to a concentrated radiation delivered by a xenon arc lamp. Pellets are oak dry cylinders of $10 \times 10^{-3} \text{ m}$ diameters and $3 \times 10^{-3} \text{ m}$ thickness (density: 760 kg.m^{-3}). The gas products (CO , CO_2 , H_2 , CH_4 and C_2H_4) formed during the devolatilization are recovered in a sampling bag and analyzed by gas chromatography. The pellet mass is measured before and after the heating time. Such experiments have been already described in details in (Authier et al., 2009) and (Authier and Lédé, 2013).

4.2 Modeling

Figure 3 shows a quite good agreement between experimental mass loss and modeling results. The mean composition of gas phase is also quite well predicted (Figure 4), especially at higher available heat flux density. Gas composition at thermodynamic equilibrium is also displayed in Figure 4.a. showing that gas composition during devolatilization is clearly out of equilibrium.

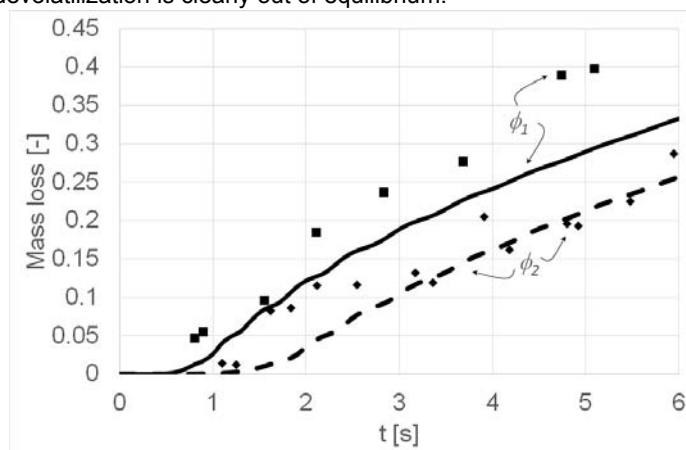
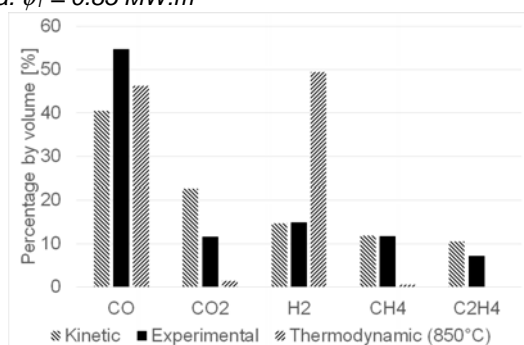


Figure 3: Variation of mass loss as a function of time for two values of the available heat flux density ($\phi_1 = 0.85 \text{ MW.m}^{-2}$ and $\phi_2 = 0.55 \text{ MW.m}^{-2}$, points: experiments, lines: model results)

a. $\phi_1 = 0.85 \text{ MW.m}^{-2}$



b. $\phi_2 = 0.55 \text{ MW.m}^{-2}$

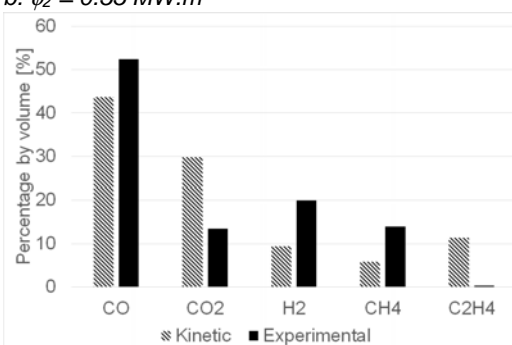


Figure 4: Gas composition for two values of the available heat flux density under image furnace conditions

5. Conclusion

From an engineering point of view, the great interest of a predictive detailed model based on standard biomass properties is that the number of input parameters for any biomass fuel is reduced. Such an approach seems very promising in the case of fluidized bed boilers or gasifiers that can recover a multitude of complex biomass fuels. Our results obtained under fluidized bed and image furnace conditions also highlight that modeling of biomass thermal properties can improve the devolatilization modeling in thermally thick regime.

In terms of future prospects, it is important to consider that inorganics inside biomass can affect significantly both yields and release rates of products, e.g. the conversion of bridges into char links catalyzed by inorganics. Experimental characterization is consequently still necessary to better assess and model the impact of inorganics on biomass devolatilization.

References

- Aarsen F.G. van den, 1985. Fluidised Bed Wood Gasifier Performance and Modeling (dissertation). Technische Hogeschool Twente, The Netherlands.
- Agarwal P.K., 1991. Transport phenomena in multi-particles systems-IV. Heat transfer to a large freely moving particle in gas fluidized bed of smaller particles. *Chem. Eng. Sci.*, 46, 1115-1127.
- Authier O., Ferrer M., Mauviel G., Khalfi A.-E., Lédé J., 2009. Wood Fast Pyrolysis: Comparison of Lagrangian and Eulerian Modeling Approaches with Experimental Measurements. *Ind. Eng. Chem. Res.*, 48, 4796-4809.
- Authier O., Lédé J., 2013. The image furnace for studying thermal reactions involving solids. Application to wood pyrolysis and gasification, and vapours catalytic cracking. *Fuel*, 107, 555-569.
- Coimbra C.F.M., Queiroz M., 1995. Evaluation of a Dimensionless Group Number to Determine Second-Einstein Temperatures in a Heat Capacity Model for All Coal Ranks. *Combust. Flame*, 101, 209-220.
- Dupont C., Chiriac R., Gauthier G., Toche F., 2014. Heat capacity measurements of various biomass types and pyrolysis residues. *Fuel*, 115, 644-651.
- Grønli M.G., 1996. A theoretical and experimental study of the thermal degradation of biomass (dissertation). Norwegian University of Science and Technology, Trondheim, Norway.
- Gupta M., Yang J., Roy C., 2003. Specific heat and thermal conductivity of softwood bark and softwood char particles. *Fuel*, 82, 919-927.
- Harada T., Hata T., Ishihara S., 1998. Thermal constants of wood during the heating process measured with the laser flash method. *J. Wood Sci.*, 44, 425-431.
- Larfeldt J., Leckner B., Melaaen M.C., 2000. Modelling and measurements of heat transfer in charcoal from pyrolysis of large wood particles. *Biomass Bioenergy*, 18, 507-514.
- Merrick D., 1983. Mathematical models of the thermal decomposition of coal: 2. Specific heats and heats of reaction. *Fuel*, 62, 540-546.
- Niksa S., 2000. Predicting the rapid devolatilization of diverse forms of biomass with bio-flashchain. *Proc. Combust. Inst.*, 28, 2727-2733.
- Ranzi E., Corbetta M., Manenti F., Pierucci S., 2014. Kinetic modeling of the thermal degradation and combustion of biomass. *Chem. Eng. Sci.*, 110, 2-12.
- Ranzi E., Cuoci A., Faravelli T., Frassoldati A., Migliavacca G., Pierucci S., Sommariva S., 2008. Chemical Kinetics of Biomass Pyrolysis. *Energy Fuels*, 22, 4292-4300.
- Rapagnà S., Mazziotti di Celso G., 2008. Devolatilization of wood particles in a hot fluidized bed: Product yields and conversion rates. *Biomass Bioenergy*, 32, 1123-1129.
- Sheng C., Azevedo J.L.T., 2002. Modeling biomass devolatilization using the chemical percolation devolatilization model for the main components. *Proc. Combust. Inst.*, 29, 407-414.
- Sreekanth M., Kolar A.K., 2010. Mass loss and apparent kinetics of a thermally thick wood particle devolatilizing in a bubbling fluidized bed combustor. *Fuel*, 89, 1050-1055.
- Sudhakar D.R., Kolar A.K., 2011. Experimental investigation of the effect of initial fuel particle shape, size and bed temperature on devolatilization of single wood particle in a hot fluidized bed. *J. Anal. Appl. Pyrolysis*, 92, 239-249.
- Thunman H., Leckner B., 2002. Thermal conductivity of wood—models for different stages of combustion. *Biomass Bioenergy*, 23, 47-54.